Energy &
Environmental Science

Supporting Information for

Solution-Processed Small Molecule:Fullerene Bulk-Heterojunction Solar Cells: Impedance Spectroscopy Deduced Bulk and Interfacial Limits to Fill-Factor.

By *Antonio Guerrero, Stephen Loser, Germà Garcia-Belmonte, Carson J. Bruns, Jeremy Smith, Hiroyuki Miyauchi, Samuel I. Stupp, Juan Bisquert*, and Tobin J. Marks**

1. Experimental Details

1.1. Materials

The following materials and reagents were purchased and used as received: **P3HT** (Luminescence Technology Corp.), [6,6]-phenyl-C_{61}-butyric acid methyl ester ($PC_{61}BM$, Nano-C or American Dye Source), while *n*-butyllithium (2.5 M in hexanes), $SnBu_3Cl$ and $Pd(PPh_3)_4$ were purchased from Sigma-Aldrich. N-bromosuccinimide (NBS) was also purchased from Sigma-Aldrich and recrystallized from H_2O. Anhydrous $CHCl_3$, anhydrous o-dichlorobenzene, anhydrous THF, $CDCl_3$, $CHCl_3$, DMF, EtOAc, hexanes, MeOH, and PhMe were purchased from Sigma-Aldrich and used without further purification. All reactions were carried out under an inert atmosphere of N_2. Analytical thin-layer chromatography (TLC) was performed on aluminum sheets, precoated with silica gel 60-F_{254} (Merck 5554). Flash column chromatography was carried out using silica gel 60 (Silicycle) as the stationary phase. NMR spectra were recorded on Bruker Avance III 500 spectrometer, with working frequencies of 499.4 MHz for ^1H and 125.6 MHz for ^{13}C nuclei. Chemical shifts are reported in ppm and referenced to the residual non-deuterated solvent frequencies ($CDCl_3$: δ 7.27 ppm for ^1H, δ 77.0 ppm for ^{13}C). High-resolution mass spectra were recorded on an Agilent 6210 LC-TOF multimode ionization (MMI) mass spectrometer. **z-NDT(TDPP)$_2$** was synthesised using a previously reported method.[1]

Energy &
Environmental Science

1.1.1. Synthesis of BDT(TDPP)$_2$

The **BDT(TDPP)$_2$** donor has not been reported previously and was synthesized via Pd-catalyzed Stille cross coupling of BDT($SnBu_3$)$_2$ and DPPBr in 67% yield (**Scheme SI1a**). **BDT($SnBu_3$)$_2$**: Dry THF (15 mL) was added to BDT (410 mg, 0.92 mmol) in a flame-dried flask and stirred at –70 °C in an acetone/dry ice bath for 30 min. A 2.5 M solution of *n*-butyllithium (920 μL, 2.3 mmol) in hexanes was added dropwise. The reaction stirred at –70 °C for 30 min and at ambient temperature for 30 min, forming a white precipitate. The reaction was cooled to –70 °C and $SnBu_3Cl$ (750 μL, 2.8 mmol) was added dropwise, during which time the precipitate disappeared. The reaction was stirred at ambient temperature overnight, quenched with H_2O (50 mL), and extracted with hexanes (2×50 mL). The organic layer was concentrated, passed through a plug of silica in hexanes, and the solvent was removed to afford the title compound as a yellow liquid (830 mg, 88%).^{1}H NMR (500 MHz, $CDCl_3$, 298 K): δ = 7.51 (s, 2H), 4.21 (d, J = 5.5 Hz, 4H), 1.82 (septet, J = 6.0 Hz, 2H), 1.75–1.18 (m, 52H), 1.04 (t, J = 7.5 Hz, 6 H), 0.97–0.89 (m, 24H) ppm. ^{13}C NMR (125 MHz, $CDCl_3$, 298 K): δ = 143.0, 139.7, 134.0, 132.8, 128.1, 75.5, 40.6, 30.5, 29.2, 29.0, 27.3, 23.9, 23.2, 14.2, 13.7, 11.3, 10.8 ppm.

BDT(TDPP)$_2$: A solution of BDT($SnBu_3$)$_2$ (444 mg, 0.433 mmol) and **TDPPBr**[29](652 mg, 1.08 mmol) in PhMe (6 mL) and DMF (1.5 mL) was degassed with bubbling N_2 for 1.5 h, then $Pd(PPh_3)_4$ (50 mg, 0.043 mmol) was added. The reaction was heated to 120 °C and stirred for 24 h, then poured into MeOH (150 mL) and stirred for 15 min. The resulting precipitate was collected by vacuum filtration and chromatographed on SiO_2 (hexanes–$CHCl_3$, gradient from 3:2 to 1:1) to afford the title compound as a shiny, bronze-colored solid (434 mg, 67%).^{1}H NMR (500 MHz, $CDCl_3$, 298 K): δ = 9.01 (d, *J* = 4.0 Hz, 2H), 8.94 (d, *J* = 4.0 Hz, 2H), 7.65–7.64 (m, 4H), 7.47 (d, *J* = 4.0 Hz, 2H), 7.29 (dd, *J* = 5.0 Hz, 4.0 Hz, 2H), 4.23 (d, *J* = 5.5 Hz, 4H), 4.12–4.01 (m, 8H), 1.96 (septet, *J* = 6.0 Hz, 2H), 1.88 (septet, *J* = 6.0

Energy &
Environmental Science

Hz, 4H), 1.78–1.60 (m, 8H), 1.45–1.25 (m, 40H), 1.07 (t, *J* = 7.5 Hz, 6H), 0.98 (t, *J* = 7.0 Hz, 6H), 0.95 (t, *J* = 7.5 Hz, 6H), 0.91–0.86 (m, 18H) ppm. ^{13}C NMR (125 MHz, $CDCl_3$, 298 K): δ = 161.7, 144.5, 142.3, 140.4, 139.6, 136.7, 135.7, 135.5, 132.8, 130.7, 129.8, 129.6, 129.4, 128.5, 126.4, 117.7, 108.6, 108.1, 45.9, 40.6, 39.2, 39.1, 30.4, 30.2, 29.2, 28.4, 28.3, 23.8, 23.6, 23.5, 23.2, 23.1, 14.2, 14.1, 14.0, 11.3, 10.5, 10.4 ppm. HRMS (APPI-TOF-MS): *m/z* calcd for $C_{86}H_{114}N_4O_6S_6$ $[M^{\bullet}]^+$1490.7057, found 1490.7035.

1.2. Electrochemical and optical properties of pristine BDT, P3HT and z-NDT

Cyclic voltammetry of **BDT, P3HT** and **z-NDT** films was carried out to estimate the ionization potential (IP) and electronic affinity (EA) of the materials used in this study. The Ag/Ag^+ electrode was used as reference with $Bu_4N^+PF_6^-$ as the electrolyte in acetonitrile (0.1 M). Films were dropcast from $CHCl_3$ (1 mg/mL) onto a glassy carbon (8 mm^2) working electrodes and thermally treated using the same conditions as used for device fabrication. Scan rates were 50 mV/s, and IP levels are estimated from an internal Fc/Fc^+ reference, assuming an IP of 4.88 vs. vacuum.[2] For reference, the chemical structures of the compounds studied are displayed in **Figure 2a**. Cyclic voltammetry (**Figure SI1**) reveals that the oxidation potential onset (E^{onset}_{ox}) for **BDT** is shifted 0.3 V with respect to **P3HT**, indicating that the small molecule has a larger IP (5.5 eV for **BDT** vs. 5.2 eV for **P3HT**). **Z-NDT** shows intermediate IP values of 5.3eV. The optical absorption spectra of pristine **BDT, z-NDT** and **P3HT** films (**Figure SI1**) clearly show that the bandgap of the small molecule is narrower with the absorption maximum extended more toward the red region. Estimated optical bandgaps are 1.75 eV, 1.70 eV and 2.2 eV, and the EAs (e.g., the lowest occupied molecular orbital, LUMOs) are 3.7, 3.6 and 3.0 eV (inferred from the optical band gap) for **BDT, z-NDT** and **P3HT**, respectively. Optical and electrochemical data are summarized in **Table SI1**.

Energy &
Environmental Science

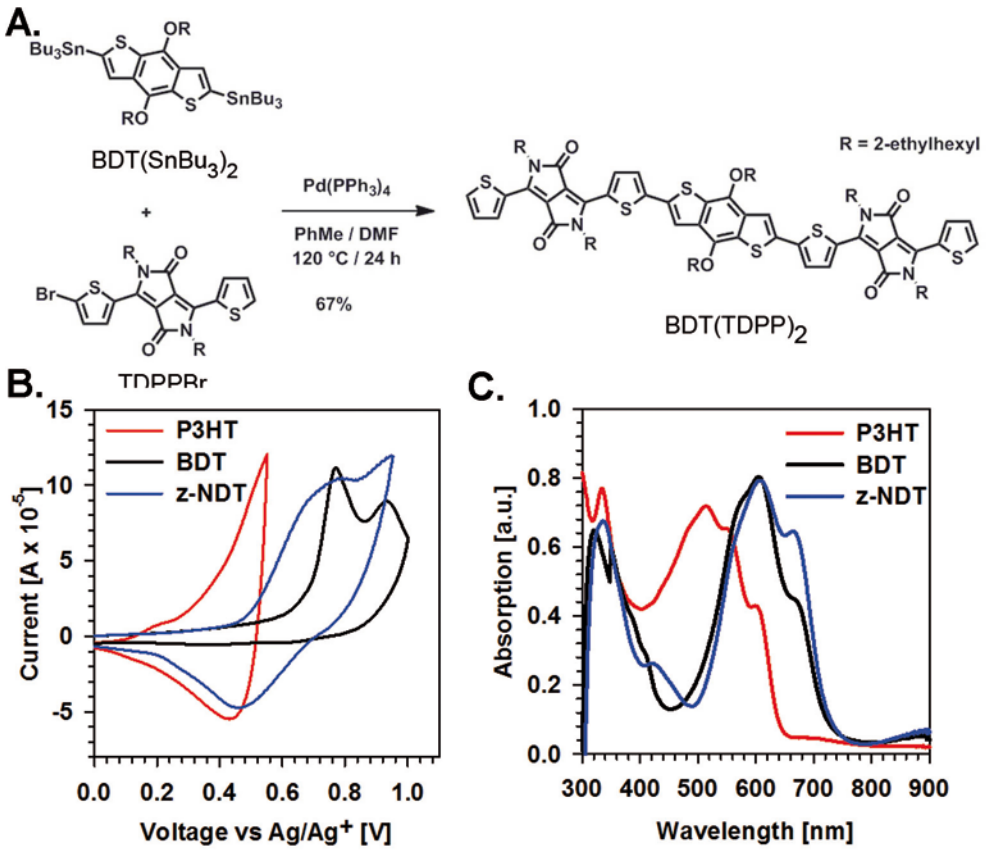

Figure SI1. (a) Donor materials P3HT and **BDT(TDPP)$_2$** (**BDT**) used in this study. (b) Cyclic voltammograms (CV) of **BDT** and **P3HT** films measured using Ag/Ag^+ as the reference electrode and $Bu_4N^+PF_6^-$ as the electrolyte in acetonitrile (0.1 M). (c) Absorption spectra of neat **BDT** and **P3HT** films.

Table SI1. IP and EA energy summary as extracted from cyclic voltammetry and film optical absorption measurements for **BDT** and **P3HT**.

Donor Material	E^{onset}_{ox} vs Ag/Ag^+ [V]	IP [eV]	EA [eV]	Bandgap [eV]
P3HT	0.12	5.2	3.0	2.2
BDT	0.45	5.5	3.7	1.8
z-NDT	0.27	5.3	3.6	1.7

2. Methods

2.1. *OPV and Hole-Only Diode Device Fabrication*

Patterned ITO-coated glass (Thin Film Device, Inc.) substrates with a resistivity of 10Ω/□ and thickness of 280 nm were cleaned by sequential sonication at 50 °C in soap/DI water, DI water, methanol, isopropanol, and acetone for 30 min. After the final sonication

step, the substrates were blown dry with a stream of N_2 gas. ITO substrates were then treated for 30 min in a UV/O_3 oven (Jelight Co.). Next, either PEDOT:PSS or MoO_3 was deposited. PEDOT:PSS (Clevios P VP Al 4083) was spun-cast at 5000 rpm for 30 sec and subsequently annealed at 150 °C for 15 min in air. Samples were then transferred to a N_2-filled glove box and an additional drying step was carried out at 100 °C for 10 min to remove traces of water. MoO_3 (Sigma-Aldrich, 99.995%) was thermally deposited at a pressure of 1.0×10^{-6} Torr at a rate of 0.1 Å/s. Prior to active layer deposition, the MoO_3 films were transferred to air for ~2 min. Active layer solutions containing donor materials and $PC_{61}BM$ were formulated inside the glove box with optimum ratios (wt:wt): **BDT(TDPP)$_2$**:$PC_{61}BM$ (1.5:1.0 in chloroform; 7 mg/mL) and **P3HT**:$PC_{61}BM$ (1:0.8 in o-dichlorobenzene; 20 mg/mL). Active layer solutions were then allowed to stir at 600 – 800 rpm for ~1 h at 45°C. The **BDT(TDPP)$_2$**:$PC_{61}BM$ active layer solutions were spun-cast between 13 – 66 rps for 20 sec after passing the solution through a 0.22 µm PTFE filter to afford active layers between 40 – 110 nm. **P3HT**:$PC_{61}BM$ active layer solutions were spun at 13 rps for 30 sec, followed by a 1 hr slow drying in a Petri dish. Samples were then thermally annealed for 10 min on a temperature-controlled hot plate at 130 °C. To finish device fabrication, Ca(5.0 nm)/Ag(100 nm) were thermally evaporated, sequentially, at a base pressure of ~1.0×10^{-6} Torr. The top Ca/Ag electrodes were then encapsulated with uv-curable epoxy and a glass slide before testing. Each substrate had 4 cells with a defined average area of 0.148 cm^2 (two cells at 0.09, one cell at 0.16, and one cell at 0.25 cm^2).

Hole-only diodes used to measure the interfacial layer transport properties were fabricated on ITO coated glass with a PEDOT:PSS hole transport layer or a MoO_3 transport layer. The BDT semiconductor was then spin coated from chloroform solution to give a film thickness, *L*, of 50 nm. Top contacts were thermally evaporated gold (50 nm) with a device area of 200x200 μm^2. The gold electrode was biased between 0 and 2 V and current measured

using a Keithley 6430 such that the ITO electrode acts as the hole collector. The current density, *J*, was then plotted as a function of applied bias (V).

2.2. *Device Characterization*

Current density-voltage and impedance spectroscopy measurements were carried out by illumination with a 1.5G illumination source (1000 W m^{-2}) using an Abet Sun 2000 Solar Simulator. The light intensity was adjusted with a calibrated Si solar cell. UV/Vis data were obtained on films using a Cary 300 Bio Spectrophotometer. External Impedance spectroscopy measurements were performed with Autolab PGSTAT-30 equipped with a frequency analyzer module, and was recorded by applying a small voltage perturbation (20 mV rms). Measurements were carried out at 1 sun light intensity at different DC bias voltage sweeping frequencies from 1 MHz down to 100 Hz. Results presented in this work are based on representative OPVs obtained from at least 4 devices (standard deviation of PCE parameters are below 5 %).

2.3. *Initial Device Optimization Using PEDOT:PSS: Optical and Photovoltaic Properties*

All devices were fabricated in the standard architecture ITO/PEDOT:PSS/Active layer/Ca/Ag The active layer comprises a blend of donor material (either **BDT** or **P3HT**, **Figure SI2a**) and the acceptor $PC_{61}BM$ ([6,6]-phenyl-C_{61}-butyric acid methyl ester) in the optimized ratios as described in the Section 2.1. The current density–voltage curves (*J*–*V*) for devices fabricated using the standard PEDOT:PSS anode IFL materials are shown in **Figure SI2a** and device parameters are described in the main text. The equivalent circuit used for systems not limited by transport of carriers in the bulk and characteristic impedance spectra is shown in **Figure SI2b** and **SI2c**, respectively.

The optical properties of the optimized blend ratios of **BDT**:$PC_{61}BM$ and **P3HT**:$PC_{61}BM$ were evaluated by measuring the steady-state film absorption (**Figure SI2d**).

$PC_{61}BM$ absorption is observed from ~300 - 350 nm and bands for the donor materials appear from 350 nm onwards. **BDT**:$PC_{61}BM$ exhibits red-shifted absorption versus **P3HT**:$PC_{61}BM$, as expected from the lower **BDT** band gap. The maximum J_{SC} was calculated by integration of the absorption spectra, accounting for the number of solar photons absorbed at each wavelength (AM 1.5G spectrum). Theoretical values of 12.2 and 11.0 mA/cm^2 are obtained for **BDT** and **P3HT**, respectively, indicating that the blend containing **BDT** can potentially provide higher currents even at smaller device thicknesses. Furthermore, external quantum efficiencies (EQEs; **Figure SI2e**) indicate a clear correlation between the film absorption profiles and the photogenerated charges extracted at each wavelength. The maximum photocurrent can also be determined from integration of the EQE curves, and the results agree very well with the measured device J_{SC} values, with theoretical values of 10.2 and 8.9 mA/cm^2 for **BDT**:$PC_{61}BM$ and **P3HT**:$PC_{61}BM$, respectively.

Energy &
Environmental Science

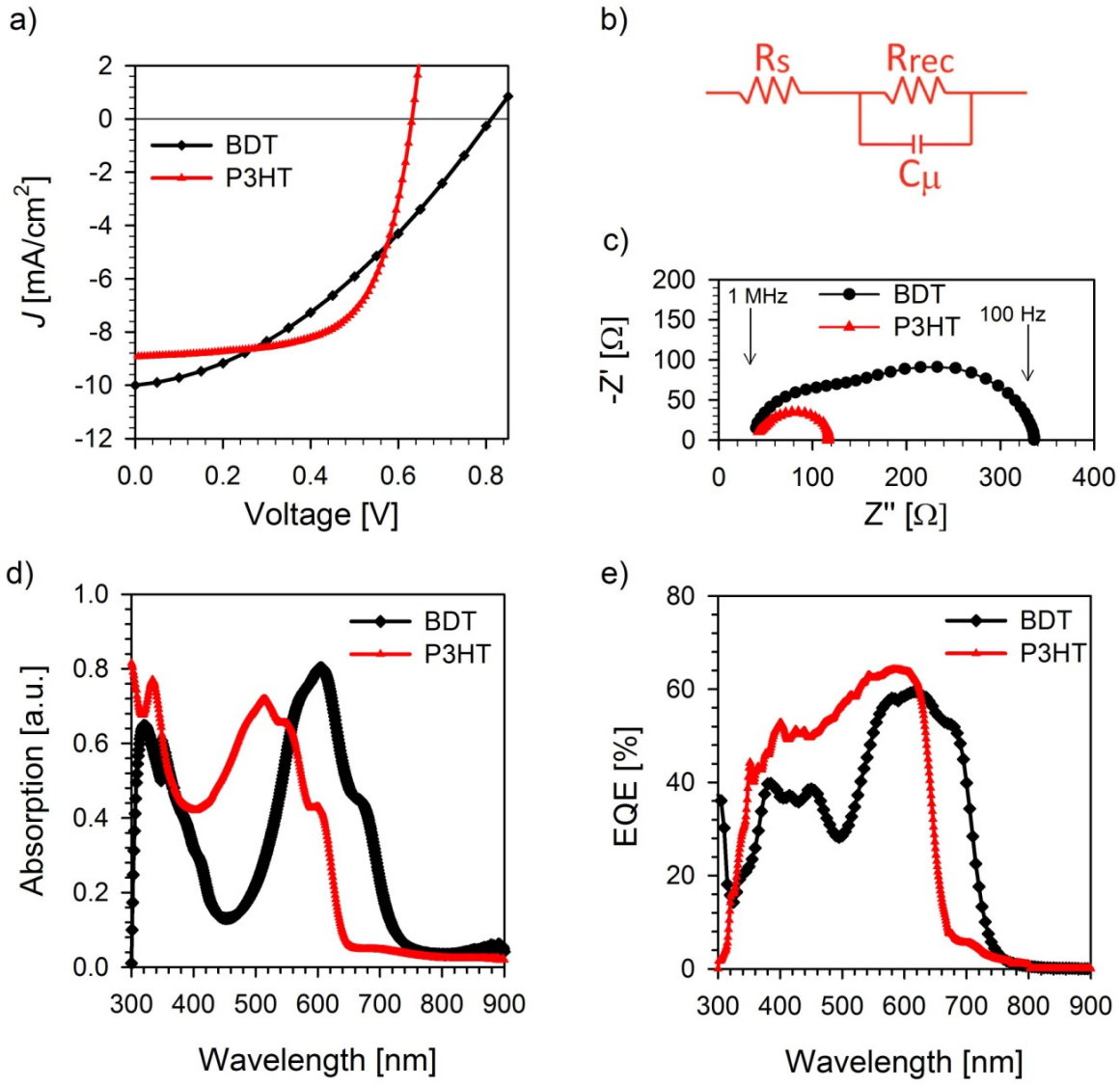

Figure SI2. (a) Measured $J-V$ response from devices using the standard device architecture: ITO/PEDOT:PSS/BHJ Active layer/Ca/Ag. (b) Equivalent circuit model used for systems not limited by transport issues such as P3HT:$PC_{61}BM$ (c) Impedance spectra of devices shown in (a) measured at 1 sun illumination and at V_{oc} conditions. Correlation between (d) blend film optical absorption and (e) external quantum efficiency (EQE) spectra of fabricated solar cells.

2.4 *Thickness Optimization of Thermally Evaporated MoO_3 IFL*

Thermally evaporated MoO_3 films were briefly exposed to air prior to spin-coating the active layer. AFM analysis (**Figure SI3a** and **SI3b**) reveals that these MoO_3 films have slightly increased rms roughnesses versus a standard PEDOT:PSS IFL. However, this does not appear to have a detrimental effect on the device response. A MoO_3 IFL thickness

optimization experiment was carried out using film thicknesses ranging from 5 nm to 20 nm, and a maximum PCE was obtained for a 5 nm MoO_3 thickness (**Figure SI3c**, Table 2). Note that the photocurrent decreases with increasing the MoO_3 thickness, in agreement with the reduced transmittance and greater resistance of the thicker MoO_3 layers (**Figure SI3d**). Note also that the J_{sc} and V_{oc} for the PEDOT:PSS and 5 nm of MoO_3 cells are comparable. More importantly, the **BDT**:$PC_{61}BM$ *FF* is greatly increased for all MoO_3 IFL cells – by up to 49 % (37% → 55%) versus a standard air-dried PEDOT:PSS IFL (**Table SI2**). In fact, as shown below, a MoO_3 anode IFL increases the PCE from 1.9 % for a PEDOT:PSS IFL using the most common drying step (air) to 3.5 %.

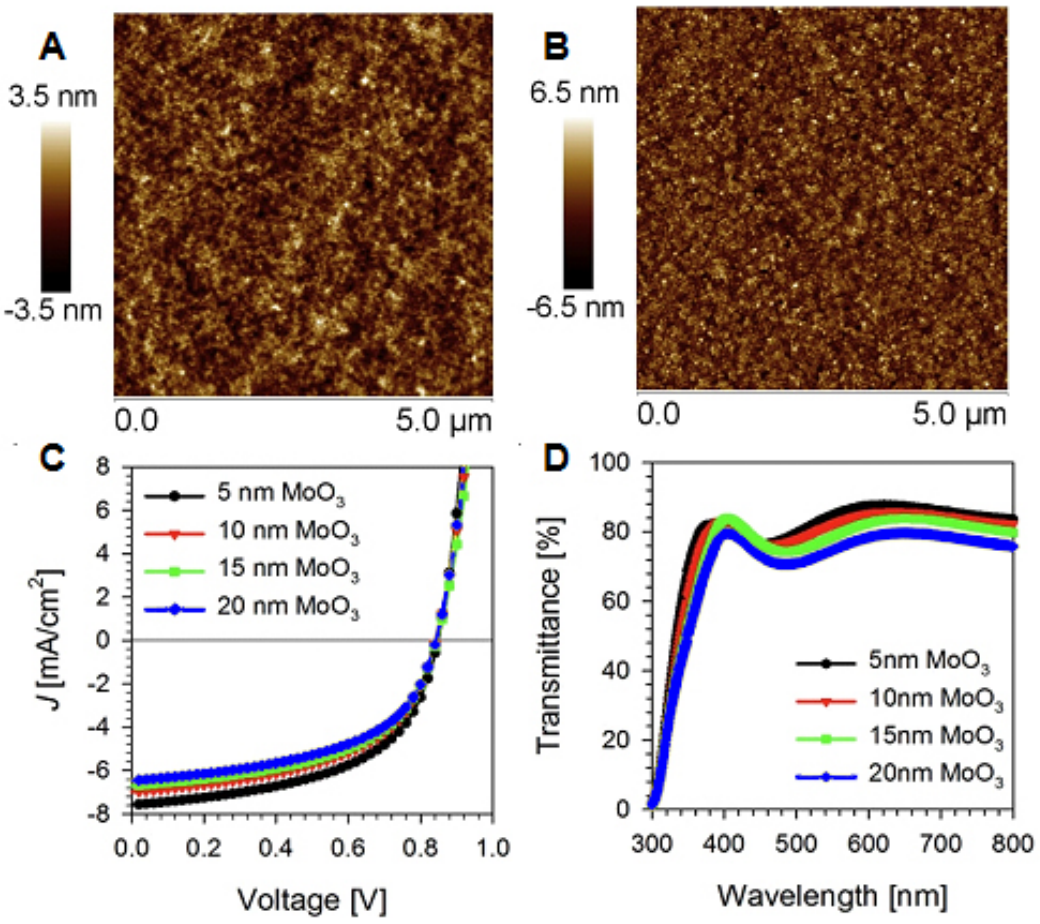

Figure SI3. AFM images of ITO substrates coated with (a) PEDOT:PSS (35 nm); RMS = 0.54 nm and (b) MoO_3 (5 nm); RMS = 0.91 nm. (c) Measured $J-V$ response from devices using the thermally evaporated MoO_3 as the IFL and **BDT**:$PC_{61}BM$ as the active layer. (d)

Energy &
Environmental Science

Transmittance spectra of MoO_3 films thermally evaporated onto ITO/glass as a function of the layer thickness.

Table SI2. Performance parameters for BHJ devices based on the absorbers **BDT** using a PEDOT:PSS anode IFL dried in the glovebox or a MoO_3 IFL having different thicknesses.

Donor Material	IFL	Active Layer Thickness [nm]	J_{SC} [mA cm^{-2}]	V_{OC} [V]	*FF* [%]	Efficiency [%]
BDT	MoO_3 (5 nm)	45	7.6	0.85	55	3.5
BDT	MoO_3 (10 nm)	45	7.0	0.84	53	3.1
BDT	MoO_3 (15 nm)	45	6.7	0.84	53	3.0
BDT	MoO_3 (20 nm)	45	6.5	0.84	53	2.9

2.5 *AFM Micrographs of OPV Active Layer*

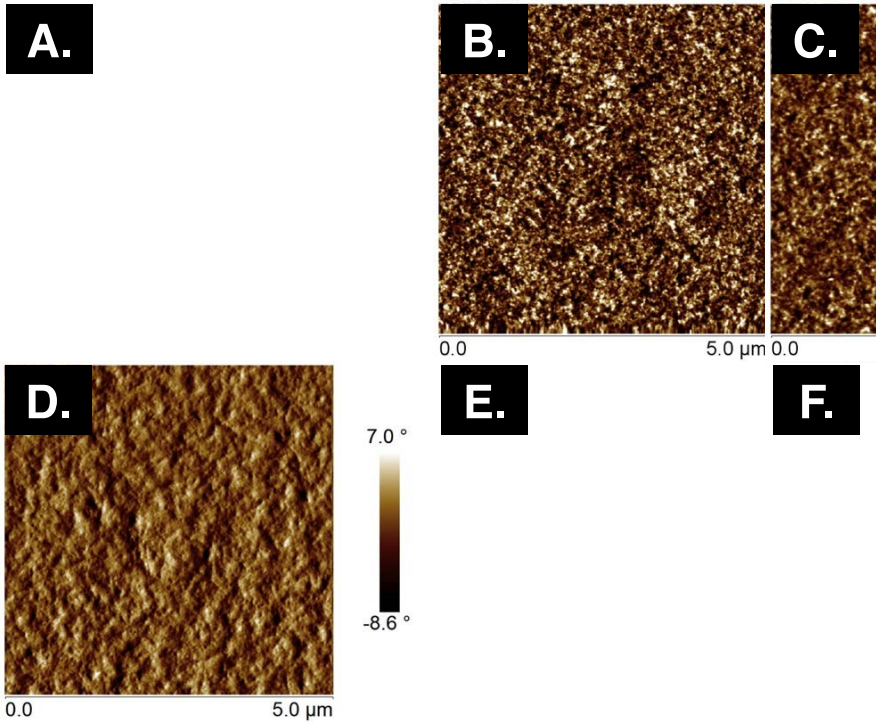

Figure SI4. Tapping mode height AFM images of the active layer morphology of (a) **P3HT**:$PC_{61}BM$ on PEDOT:PSS coated ITO, (b) **BDT**:$PC_{61}BM$ on PEDOT:PSS (air dried) coated ITO, and (c) **BDT**:$PC_{61}BM$ on thermally evaporated MoO_3 (5 nm) coated ITO, with corresponding phase images (d), (e), and (f), respectively. The RMS roughnesses for (a), (b), and (c) are 4.29, 0.87, and 0.66 nm^2, respectively. Note, each active layer was prepared exactly as it was for the OPV device conditions and each material was annealed at 130 ºC for 10 mins prior to AFM analysis.

Energy &
Environmental Science

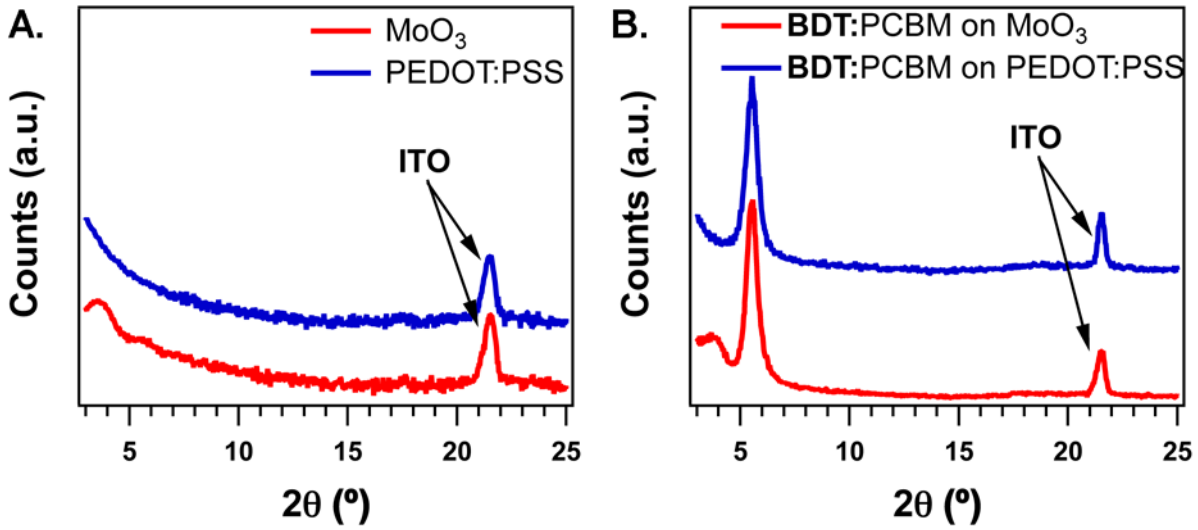

Figure SI5. XRD spectra of Glass/ITO/IFL substrates (a) and BDT:PCBM blends (b) spin casted on the top of the substrates shown on SI5a. Data suggests that the **BDT**:PCBM spin-cast film does not organize any differently on top of the MoO_3 vs. PEDOT:PSS, thus the morphology is unaffected by the choice of IFL.

References:

1. S. Loser, H. Miyauchi, J. W. Hennek, J. Smith, C. Huang, A. Facchetti and T. J. Marks, *Chem. Comm.*, 2012, 48, 8511-8513.
2. Z. B. Henson, G. C. Welch, T. van der Poll and G. C. Bazan, *Journal of the American Chemical Society*, 2012, 134, 3766-3779.